

A novel ratiometric and TURN-ON fluorescent coumarin-based probe for Fe(III)

Tiziana Pivetta^{1*}, Sebastiano Masuri¹, Maria Grazia Cabiddu¹, Claudia Caltagirone¹, Anna Pintus¹, Michela Massa¹, Francesco Isaia¹, Enzo Cadoni¹

¹ Dipartimento di Scienze Chimiche e Geologiche, Università degli Studi di Cagliari, Cittadella Universitaria, 09042 Monserrato CA – ITALY

Address reprints requests to:

Tiziana Pivetta
Dipartimento di Scienze Chimiche e Geologiche
Università degli Studi di Cagliari, Cittadella Universitaria
09042 Monserrato CA – ITALY
Tel. 0039 070 675 4473
mail: tpivetta@unica.it

Keywords Coumarin; Fe³⁺; Fluorescence; Selectivity

Supplementary Information

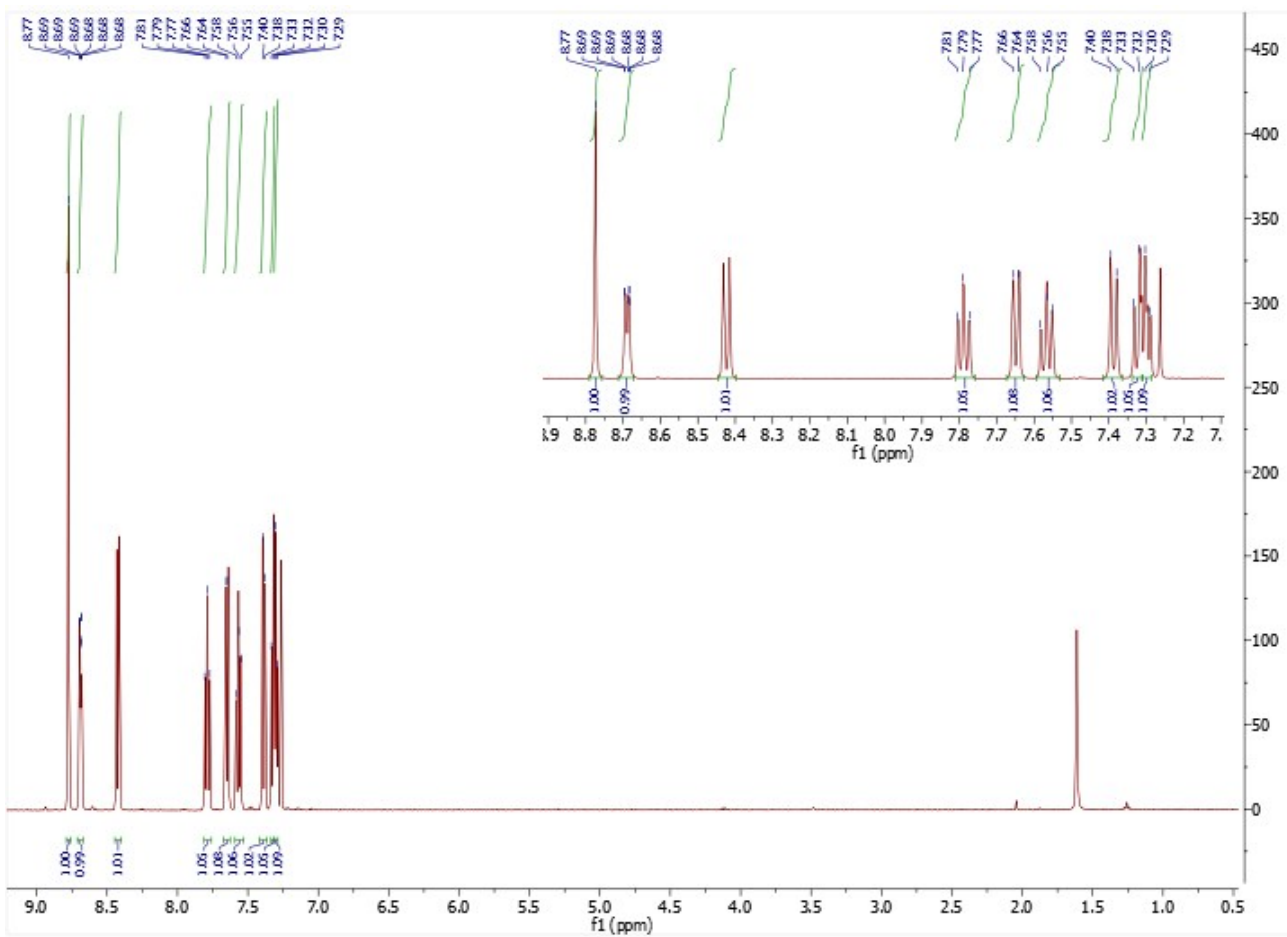


Figure S1: ^1H NMR of ligand L1, 3-(pyridin-2-yl)-2*H*-chromen-2-one. NMR spectra were recorded on a Varian 500 spectrometer at room temperature with trimethylsilane (TMS) as internal standard in CDCl_3 .

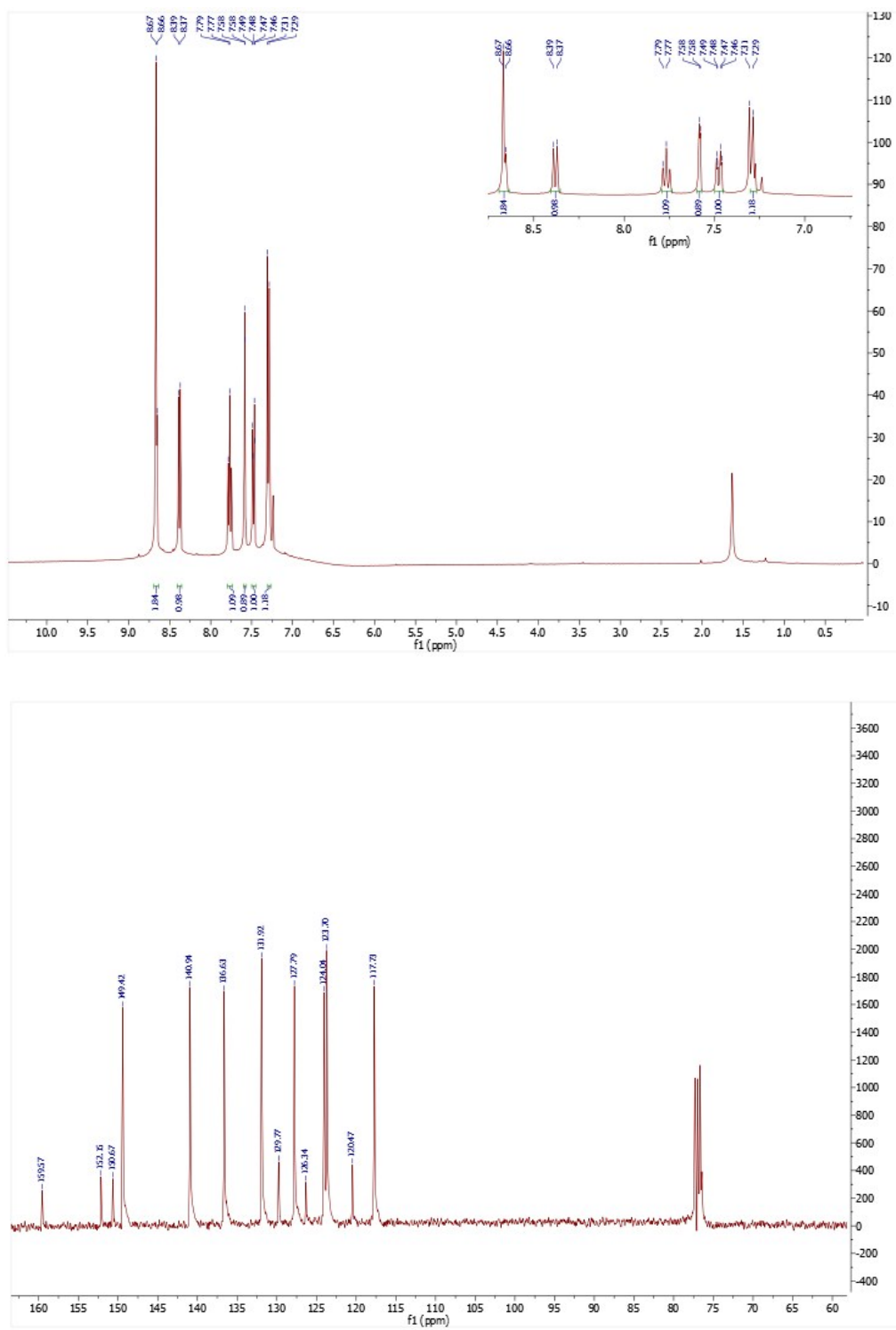


Figure S2: ^1H NMR (top) and ^{13}C NMR spectrum (bottom) of ligand L2, 6-chloro-3-(pyridin-2-yl)- $2H$ -chromen-2-one. NMR spectra were recorded on a Varian 500 spectrometer at room temperature with trimethylsilane (TMS) as internal standard in CDCl_3 .

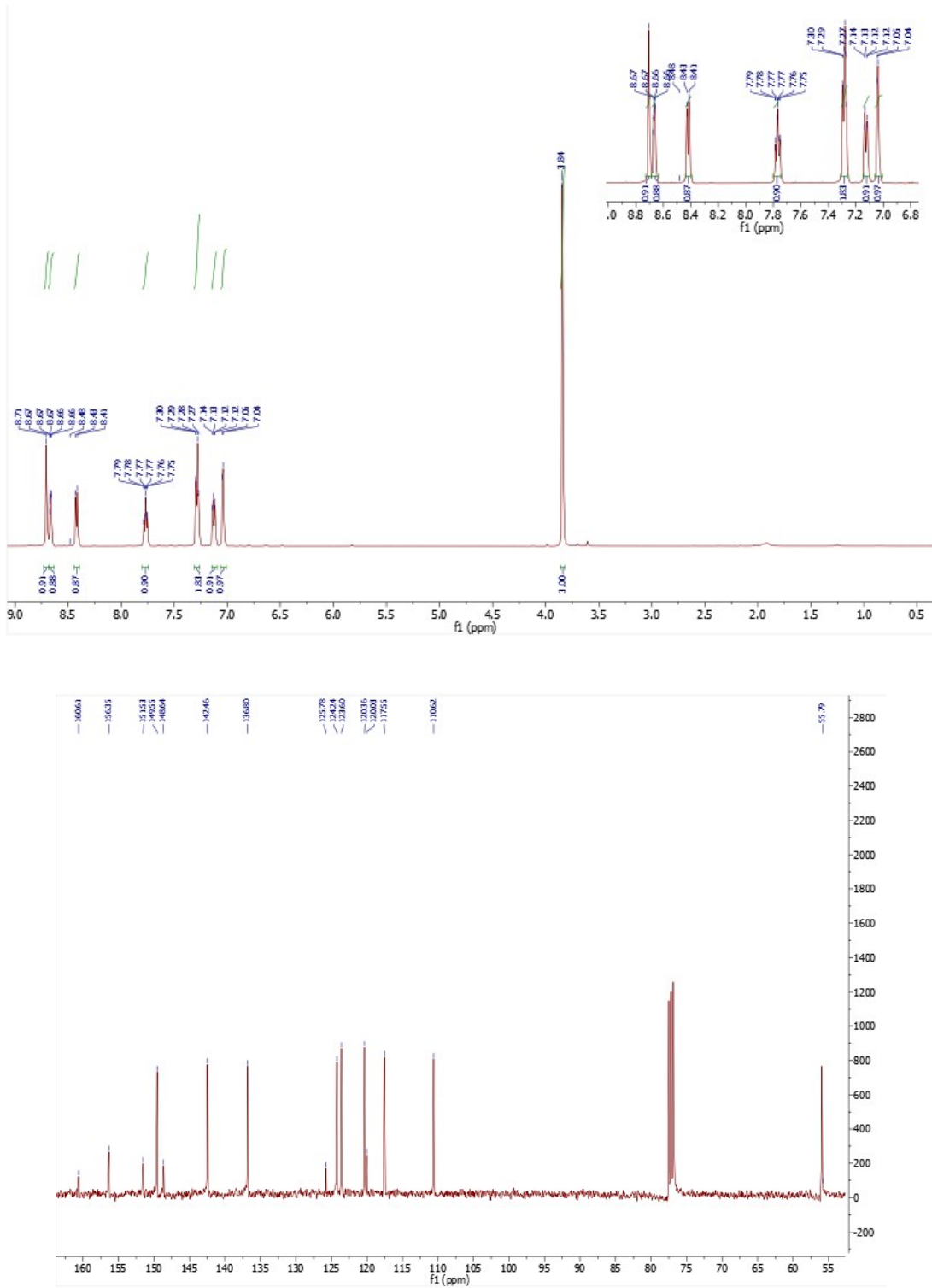


Figure S3: ^1H NMR (top) and ^{13}C NMR spectrum (bottom) of ligand L3, 6-methoxy-3-(pyridin-2-yl)-2*H*-chromen-2-one. NMR spectra were recorded on a Varian 500 spectrometer at room temperature with trimethylsilane (TMS) as internal standard in CDCl_3 .

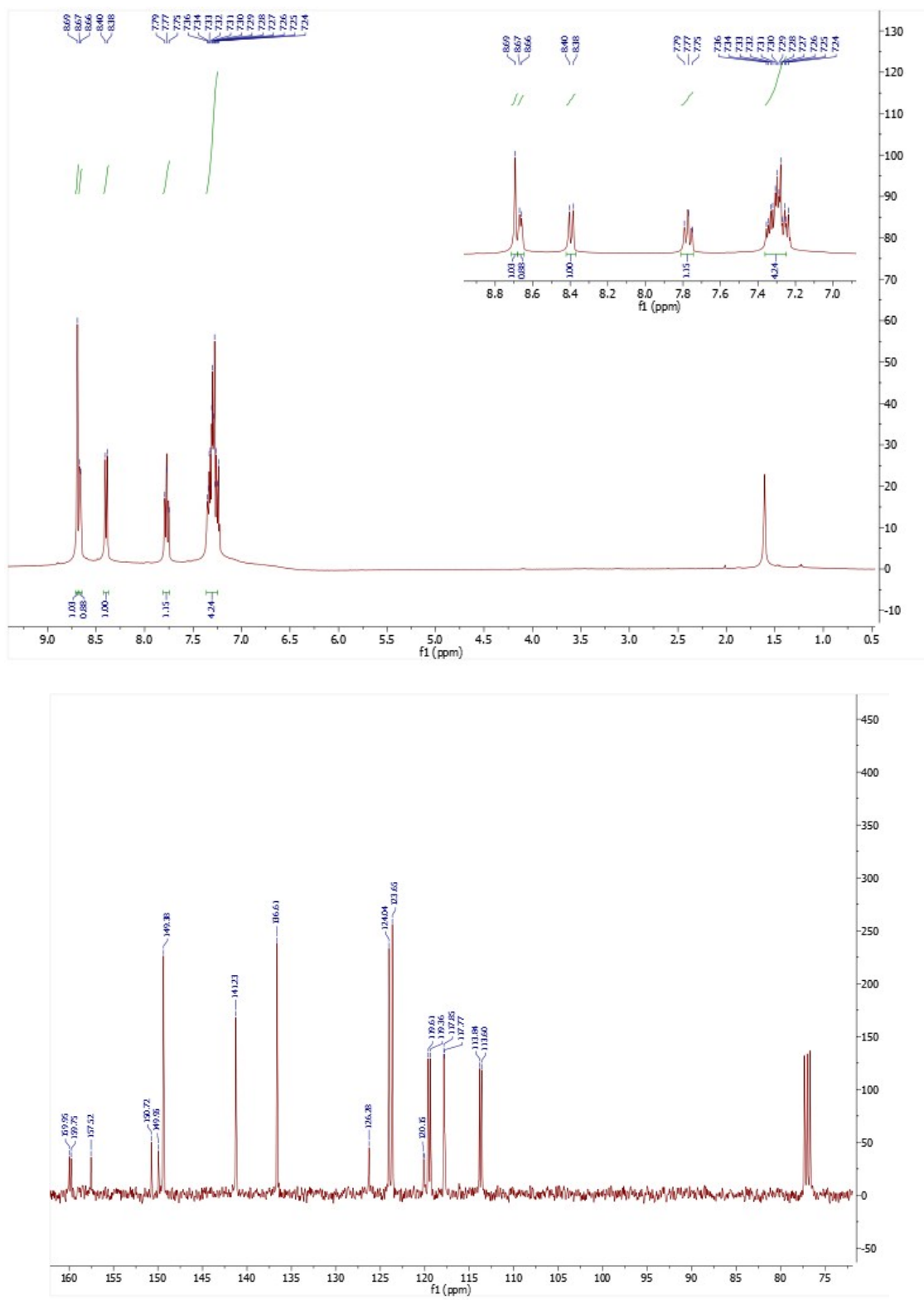


Figure S4: ¹H NMR (top) and ¹³C NMR spectrum (bottom) of ligand L4, 6-fluoro-3-(pyridin-2-yl)-2H-chromen-2-one. NMR spectra were recorded on a Varian 500 spectrometer at room temperature with trimethylsilane (TMS) as internal standard in CDCl₃.

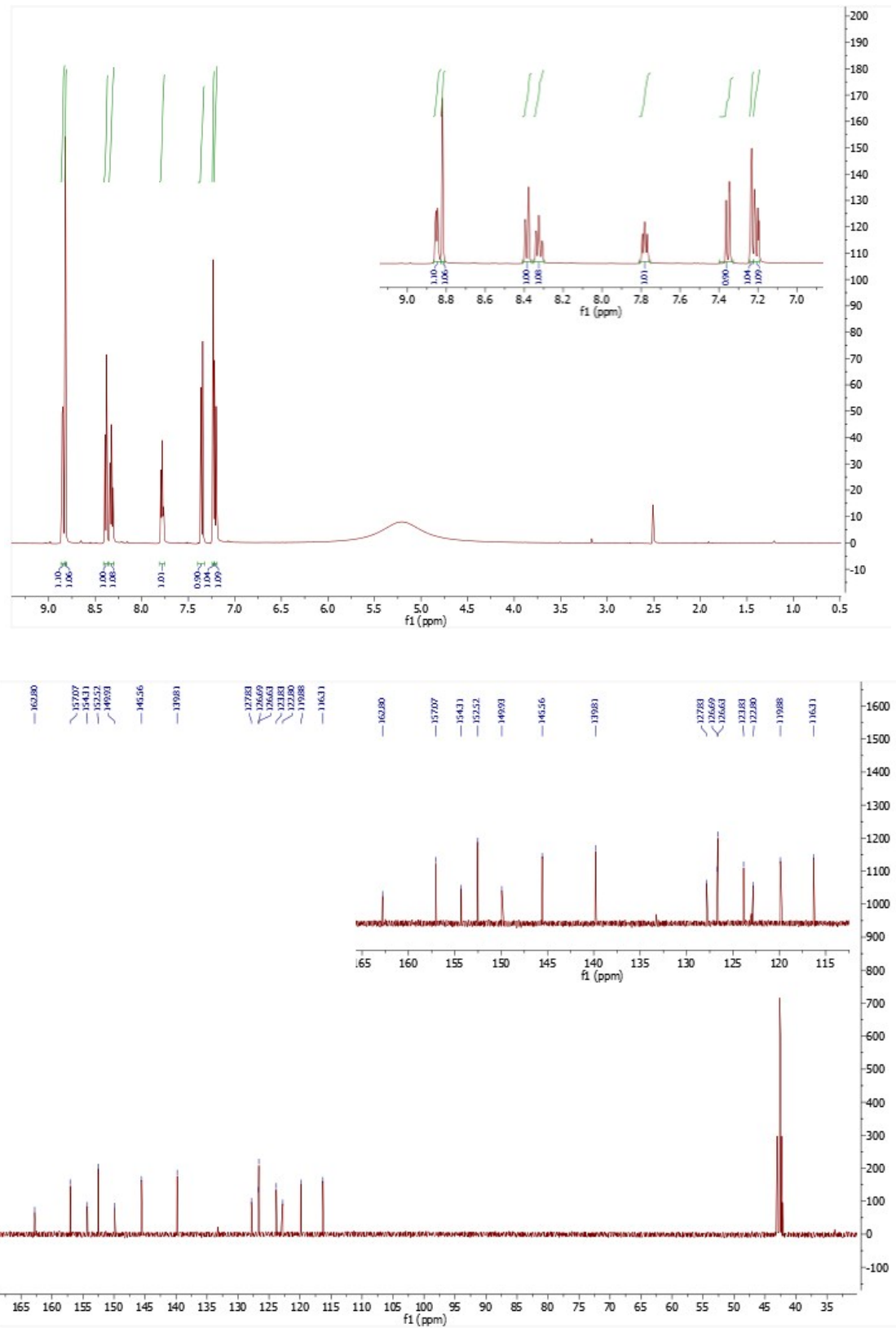


Figure S5: ^1H NMR (top) and ^{13}C NMR spectrum (bottom) of ligand L5, 6-hydroxy-3-(pyridin-2-yl)-2*H*-chromen-2-one. NMR spectra were recorded on a Varian 500 spectrometer at room temperature with trimethylsilane (TMS) as internal standard in DMSO.

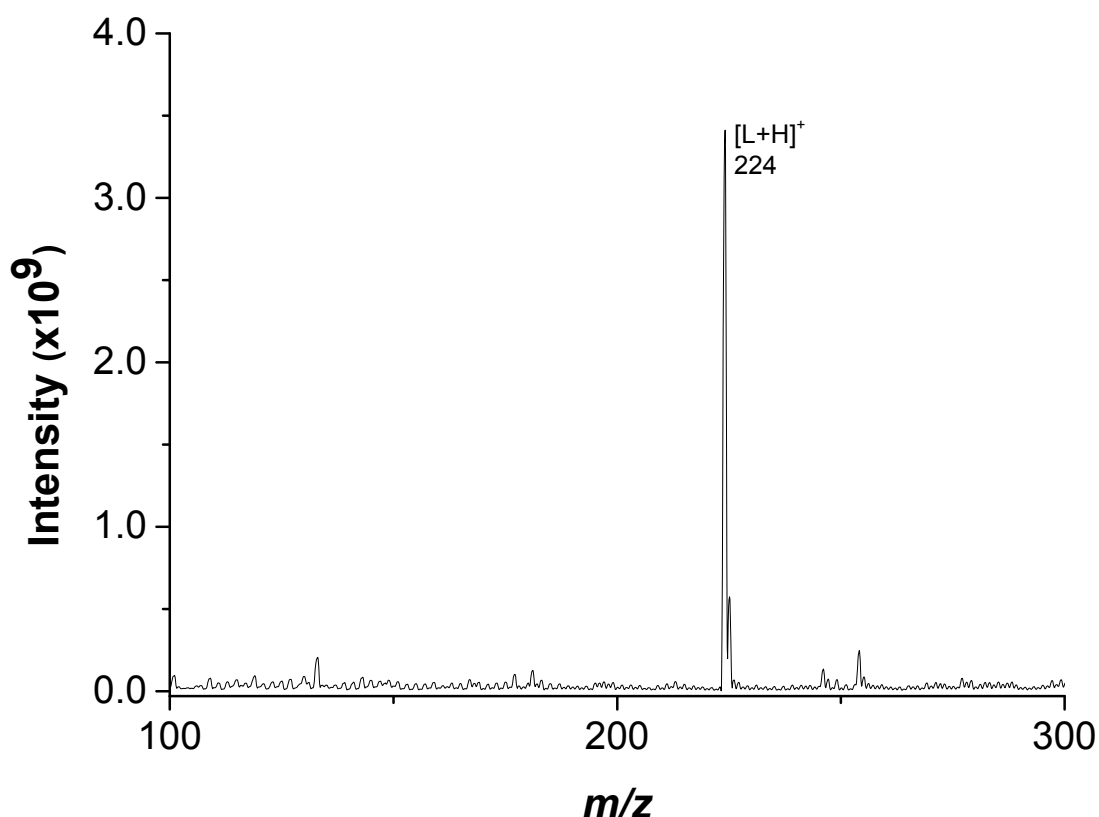


Figure S6: ESI-MS spectrum of ligand L1, 3-(pyridin-2-yl)-2*H*-chromen-2-one. Mass spectra were recorded on a triple quadruple QqQ Varian 310-MS mass spectrometer using electrospray ionisation (ESI) technique. The mass spectra were recorded in positive ion mode in the m/z 50–550 range. The experimental conditions were: needle voltage 4500 V, shield voltage 800 V, housing temperature 60 °C, drying gas temperature 150 °C, nebuliser gas pressure 40 PSI, drying gas pressure 40 PSI, and detector voltage 1650 V.

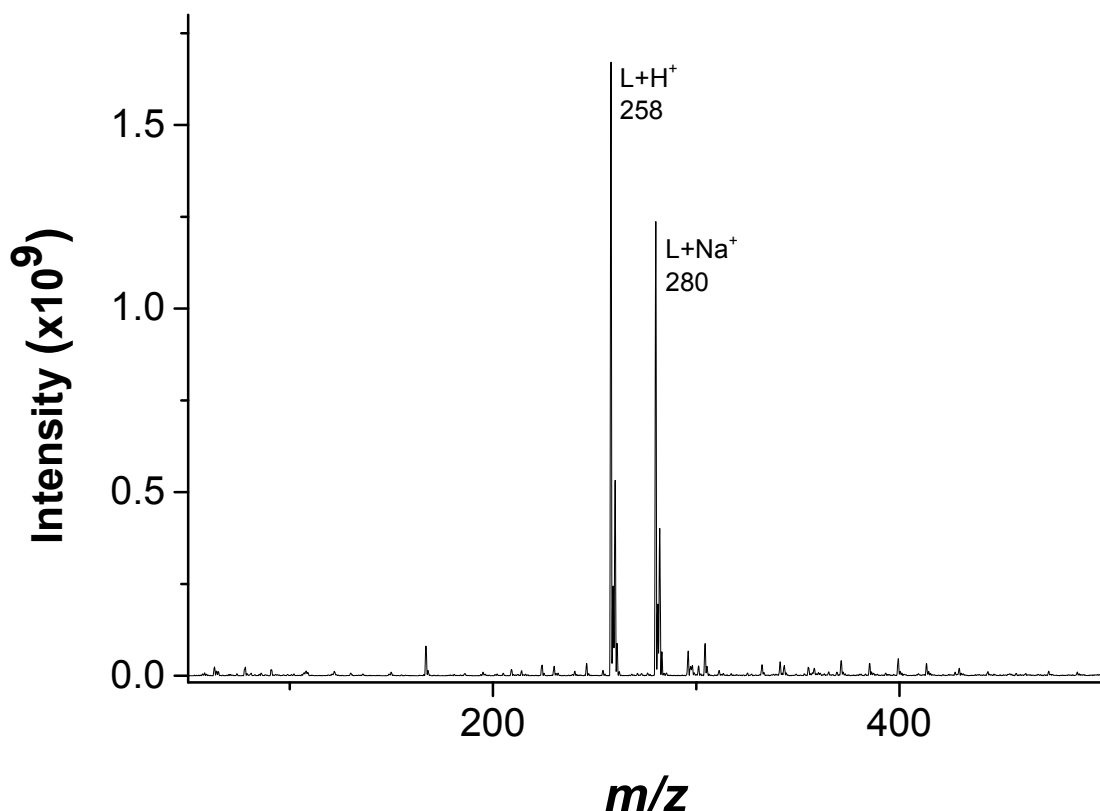


Figure S7: ESI-MS spectrum of ligand L2, 6-chloro-3-(pyridin-2-yl)-2*H*-chromen-2-one.

Mass spectra were recorded on a triple quadruple QqQ Varian 310-MS mass spectrometer using electrospray ionisation (ESI) technique. The mass spectra were recorded in positive ion mode in the m/z 50–550 range. The experimental conditions were: needle voltage 4500 V, shield voltage 800 V, housing temperature 60 °C, drying gas temperature 150 °C, nebuliser gas pressure 40 PSI, drying gas pressure 40 PSI, and detector voltage 1650 V.

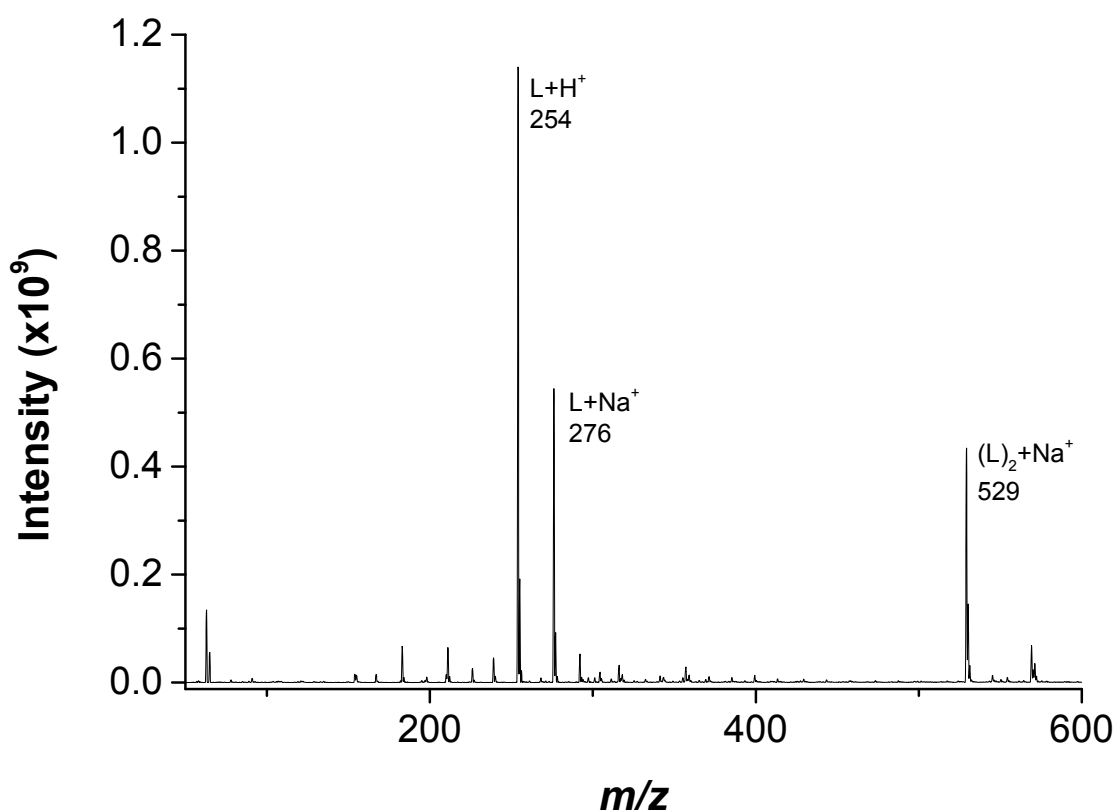


Figure S8: ESI-MS spectrum of ligand L3, 6-methoxy-3-(pyridin-2-yl)-2*H*-chromen-2-one. Mass spectra were recorded on a triple quadrupole QqQ Varian 310-MS mass spectrometer using electrospray ionisation (ESI) technique. The mass spectra were recorded in positive ion mode in the m/z 50–550 range. The experimental conditions were: needle voltage 4500 V, shield voltage 800 V, housing temperature 60 °C, drying gas temperature 150 °C, nebuliser gas pressure 40 PSI, drying gas pressure 40 PSI, and detector voltage 1650 V.

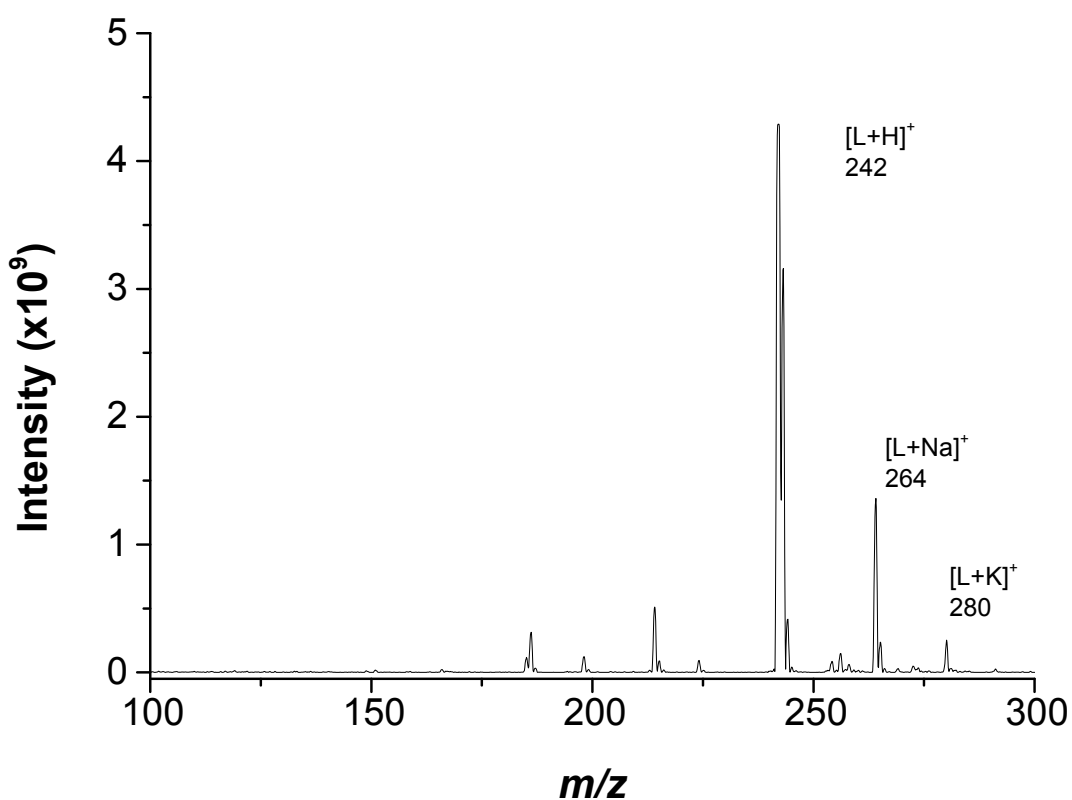


Figure S9: ESI-MS spectrum of ligand L4, 6-fluoro-3-(pyridin-2-yl)-2*H*-chromen-2-one. Mass spectra were recorded on a triple quadruple QqQ Varian 310-MS mass spectrometer using electrospray ionisation (ESI) technique. The mass spectra were recorded in positive ion mode in the m/z 50–550 range. The experimental conditions were: needle voltage 4500 V, shield voltage 800 V, housing temperature 60 °C, drying gas temperature 150 °C, nebuliser gas pressure 40 PSI, drying gas pressure 40 PSI, and detector voltage 1650 V.

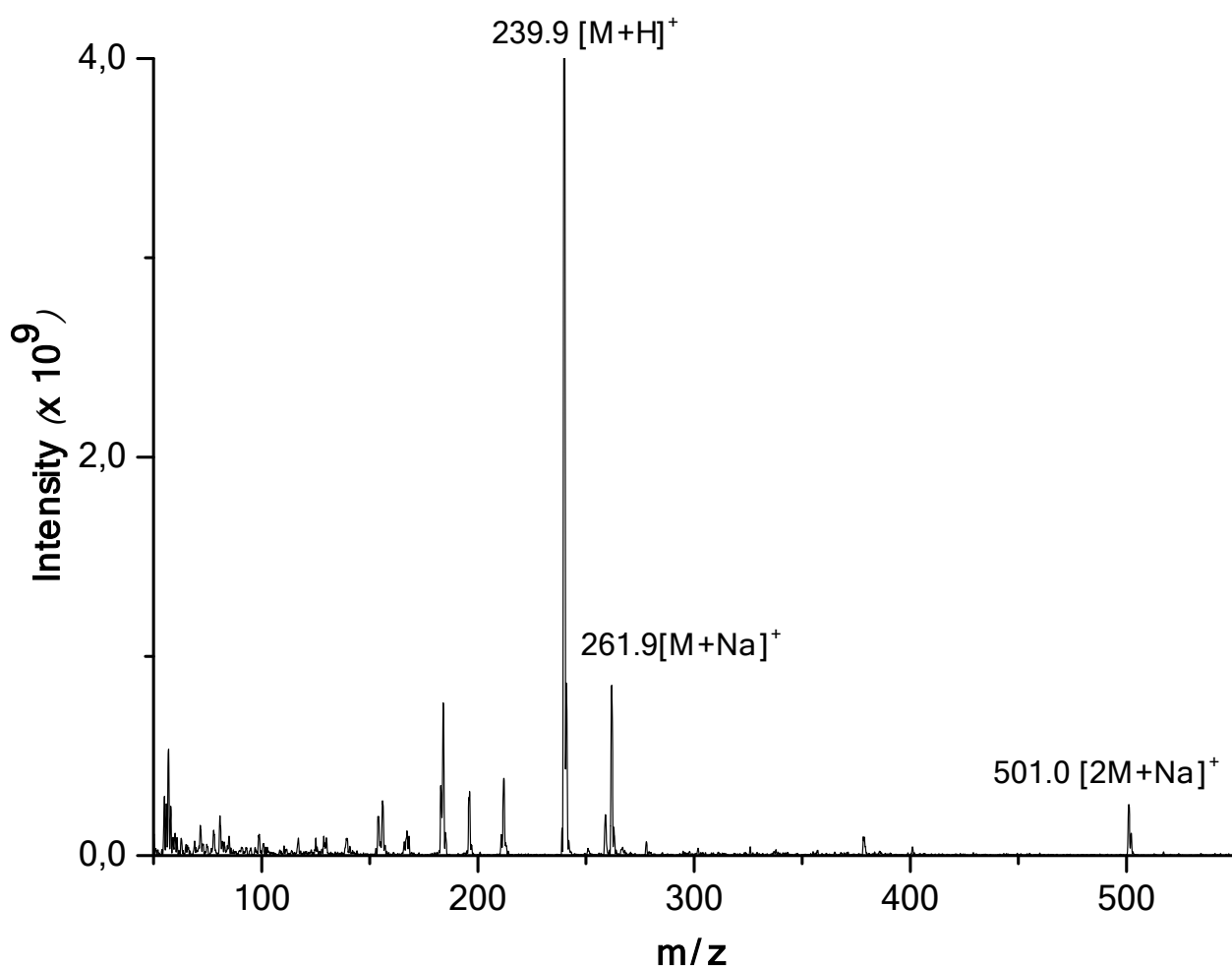


Figure S10: ESI-MS spectrum of ligand L5, 6-Hydroxy-3-(pyridin-2-yl)-2*H*-chromen-2-one. Mass spectra were recorded on a triple quadruple QqQ Varian 310-MS mass spectrometer using electrospray ionisation (ESI) technique. The mass spectra were recorded in positive ion mode in the m/z 50–550 range. The experimental conditions were: needle voltage 4500 V, shield voltage 800 V, housing temperature 60 °C, drying gas temperature 150 °C, nebuliser gas pressure 40 PSI, drying gas pressure 40 PSI, and detector voltage 1650 V.

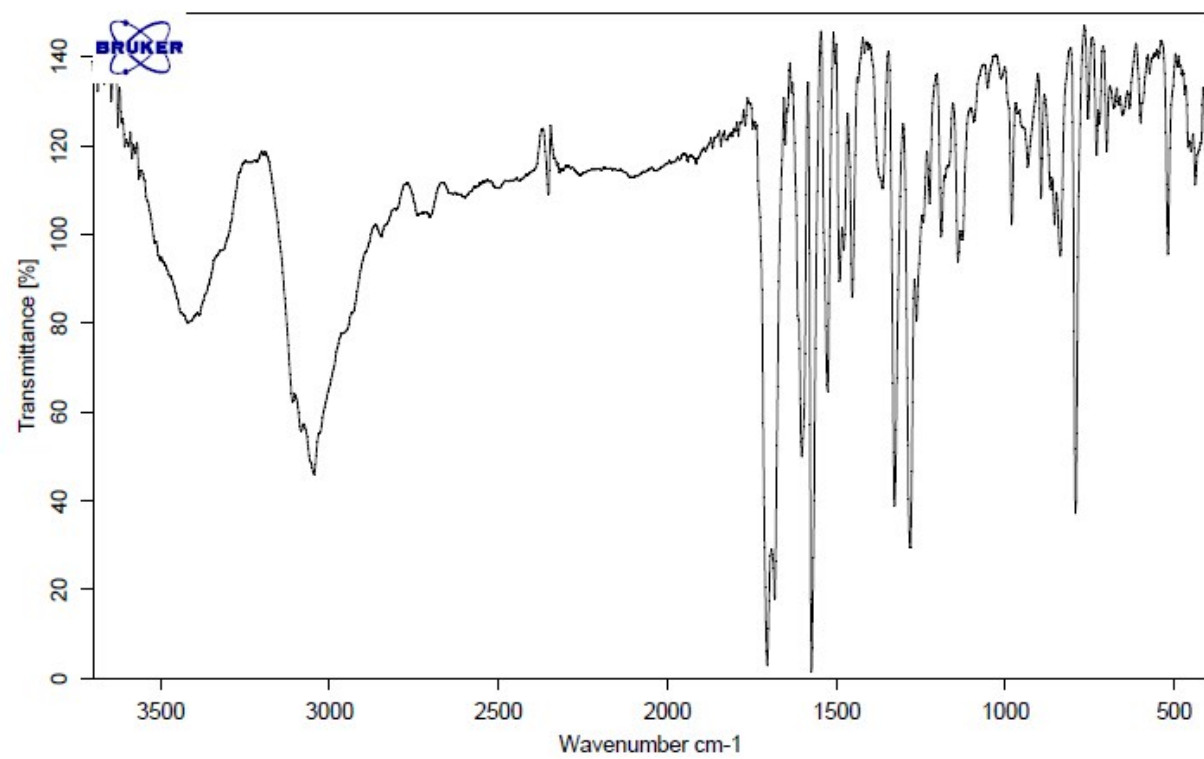


Figure S11: IR spectrum of ligand L5, 6-Hydroxy-3-(pyridin-2-yl)-2H-chromen-2-one. IR spectra were acquired with a Bruker Vector 22 spectrophotometer, preparing the samples as KBr pellets.

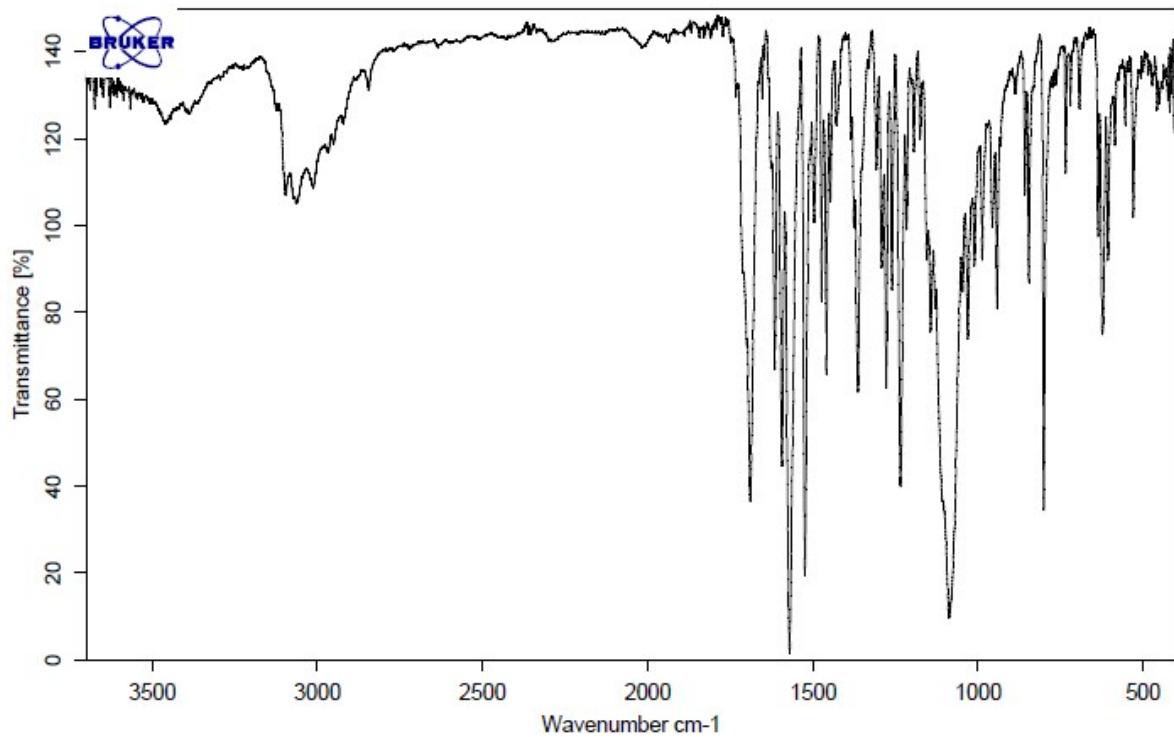
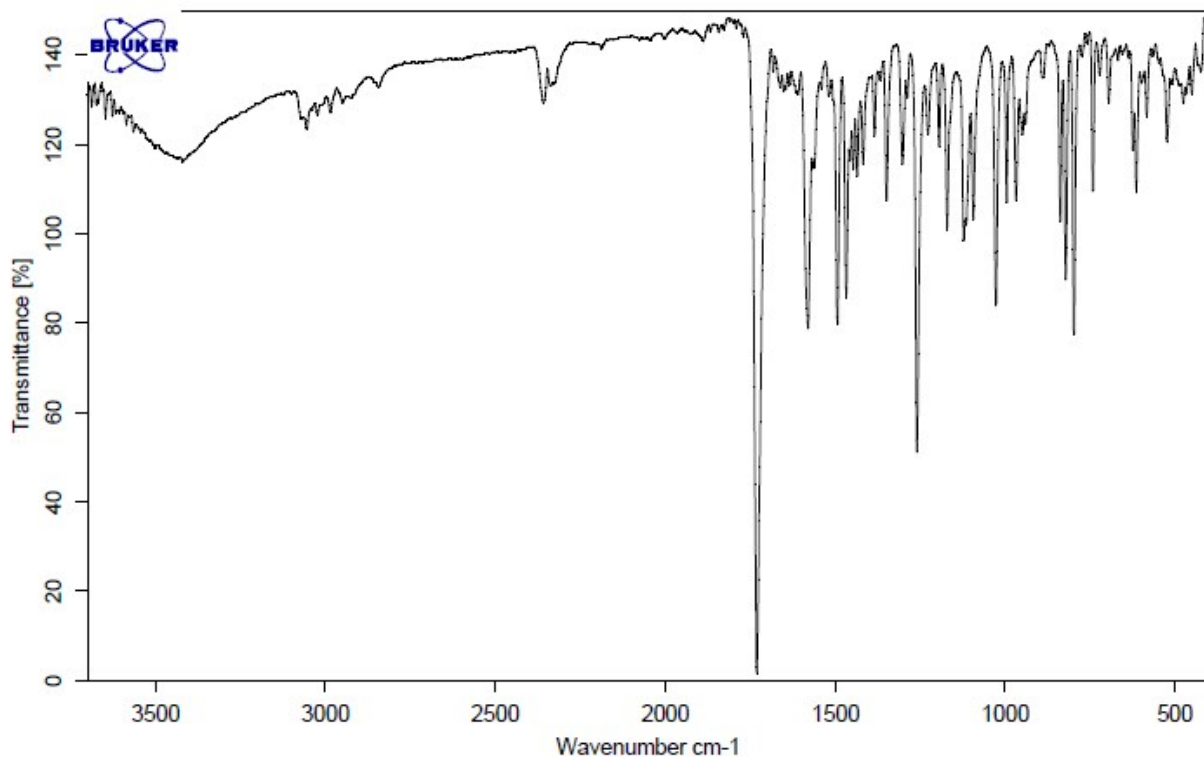


Figure S12: IR spectrum of ligand L3 (up), 6-Methoxy-3-(pyridin-2-yl)-2H-chromen-2-one and C8, $\text{Fe}(\text{L3})_3(\text{ClO}_4)_3$. (bottom). IR spectra were acquired with a Bruker Vector 22 spectrophotometer, preparing the samples as KBr pellets.

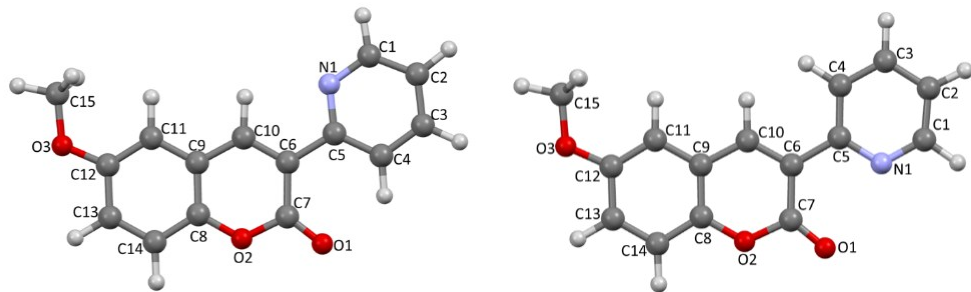


Figure S13. Molecular drawings and atom labelling schemes for **L3** in antiperiplanar (right) and periplanar (left) conformations at the DFT-optimized geometries (data are reported in Table S1)

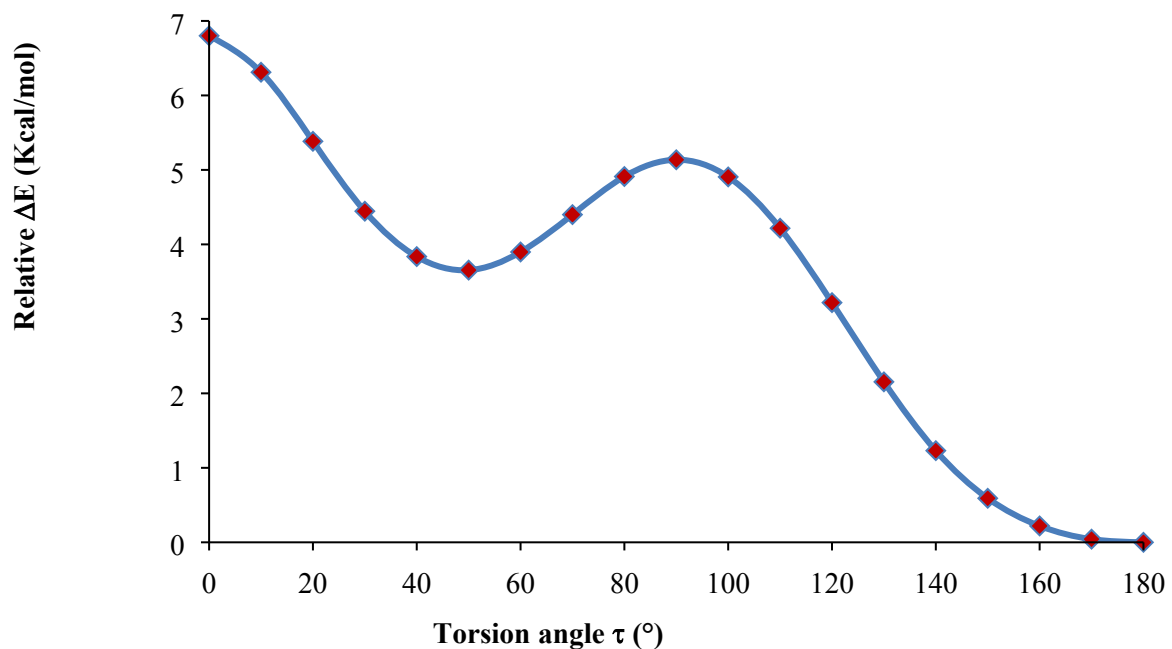


Fig. S14. Relative variation ΔE of the total electronic energy as a function of torsion angle τ (C7–C6–C5–N1 dihedral) calculated for **L3** at the DFT level.

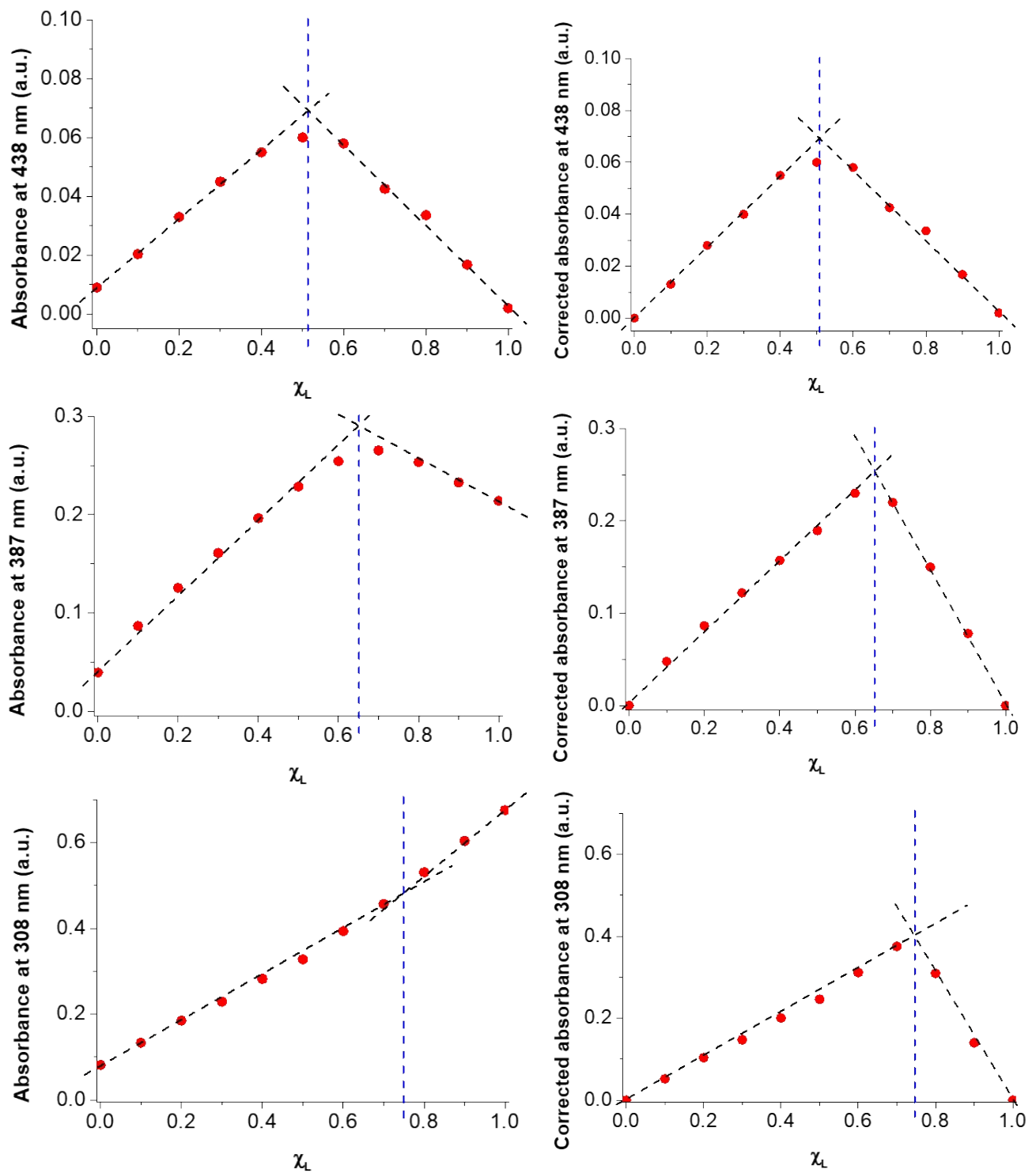


Figure S15. Job's plot for the system Fe(III)-L3. Uncorrected (left) and corrected (right) absorbances measured at different ligand:metal molar ratio at 438, 387 and 308 nm (concentration of Fe(III) = L = $5.27 \cdot 10^{-5}$ M, 0.01M NaClO₄, T 25°C, optic path length 1 cm).

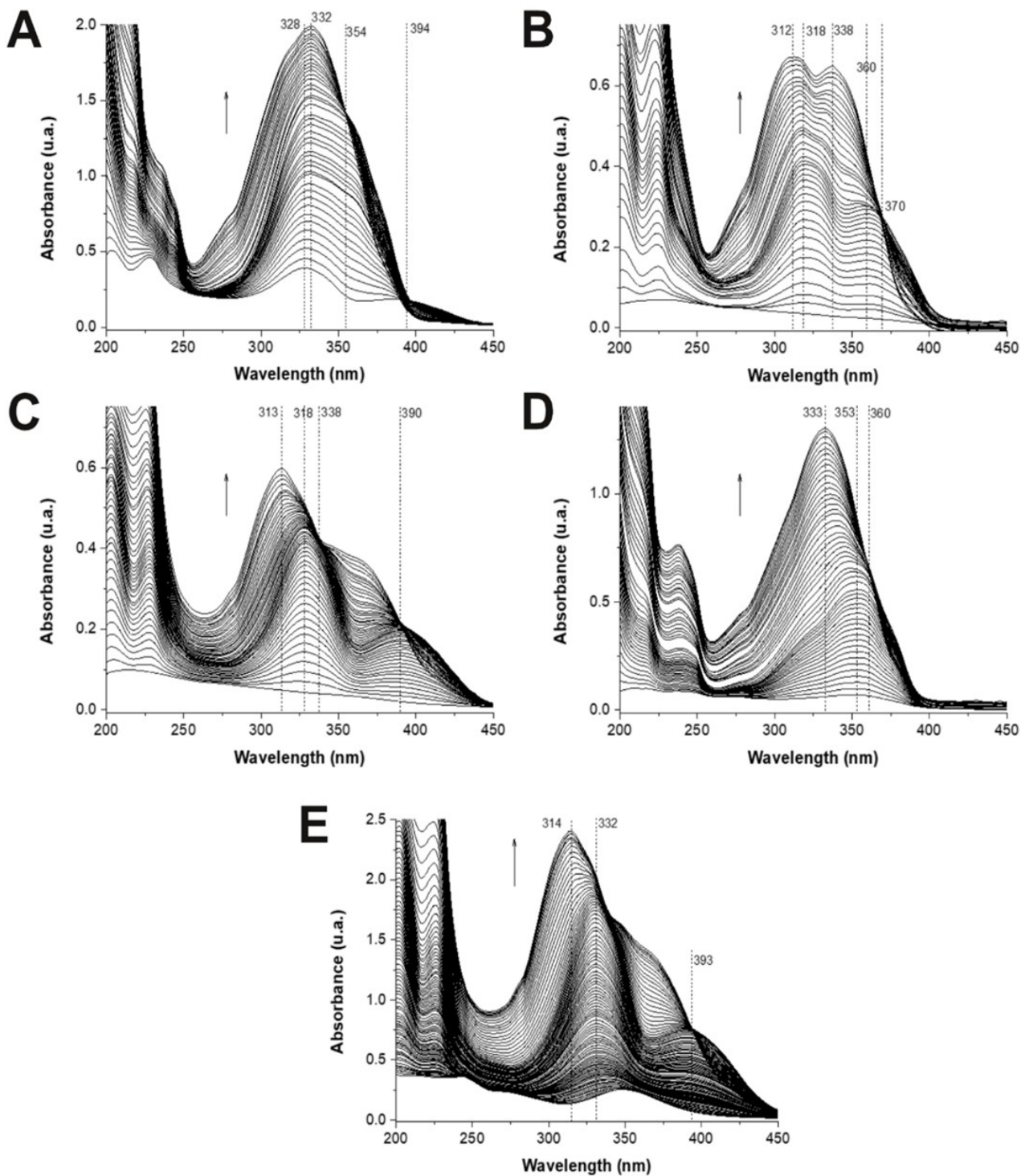


Figure S16. Selected spectra collected during the spectrophotometric titration of Fe(III) with **L1** (A) (Fe(III) $8.4 \cdot 10^{-5}$ mmoles, L $4.2 \cdot 10^{-5}$ M), **L2** (B) (Fe(III) $4.6 \cdot 10^{-5}$ mmoles, L $4.5 \cdot 10^{-5}$ M), **L3** (C) (Fe(III) $4.6 \cdot 10^{-5}$ mmoles, L $4.3 \cdot 10^{-5}$ M), **L4** (D) (Fe(III) $4.6 \cdot 10^{-5}$ mmoles, L $4.5 \cdot 10^{-5}$ M), **L5** (E) (Fe(III) $5.7 \cdot 10^{-5}$ mmoles, L $4.6 \cdot 10^{-5}$ M); NaClO₄ 0.05 M ionic strength buffer, 1 cm optical path length, 25 °C, CH₃CN solution.

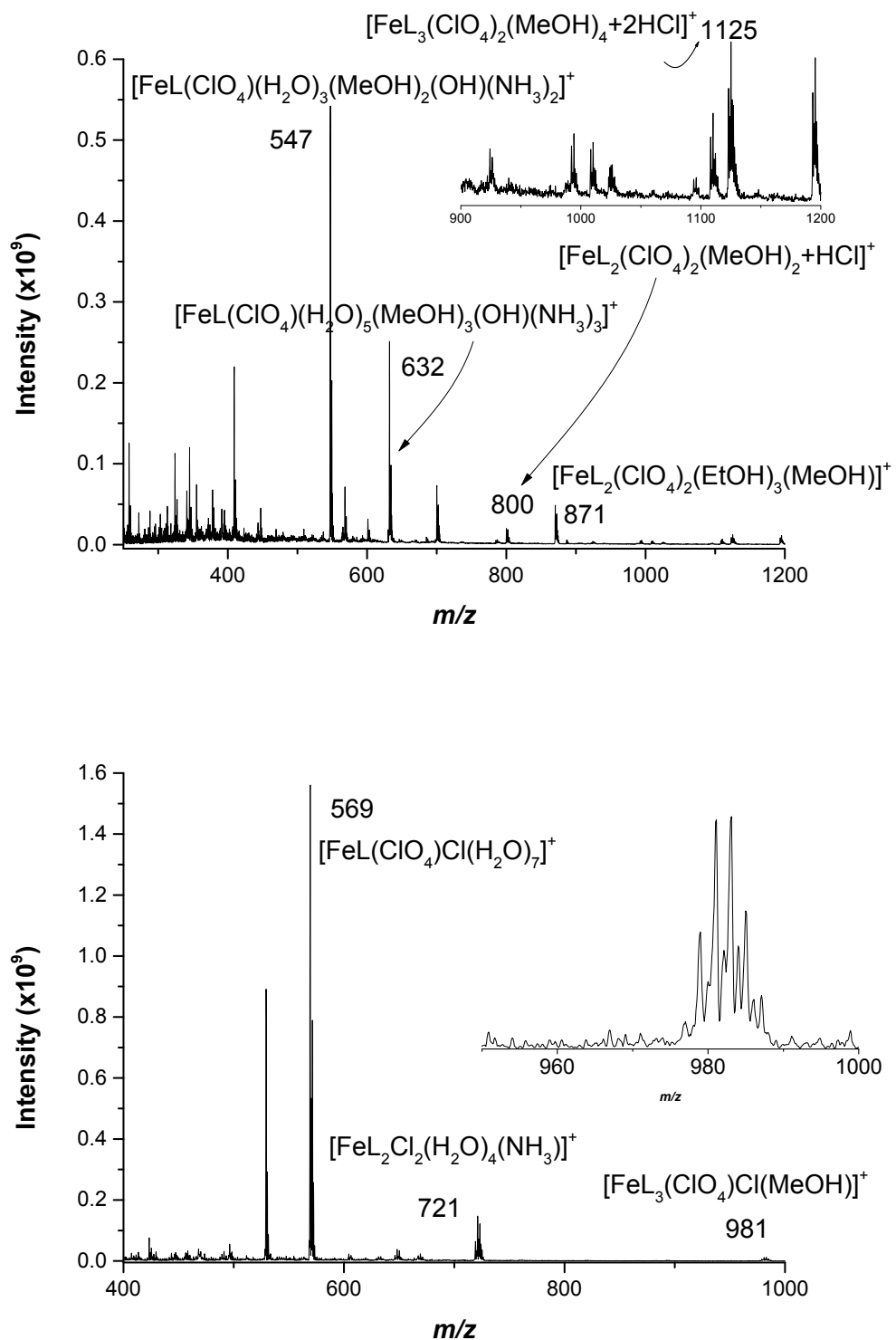


Figure S17. ESI mass spectra of solution containing Fe(III) and L1 (up) or L3 (down) in 1:3 metal:ligand molar ratio. Several adducts with solvent were evidenced. The stoichiometry was proposed on the basis of the fitting of the isotopic pattern and on MS-MS experiments (Fe(III) 1mM, H₂O:MeOH:EtOH 50:40:10).

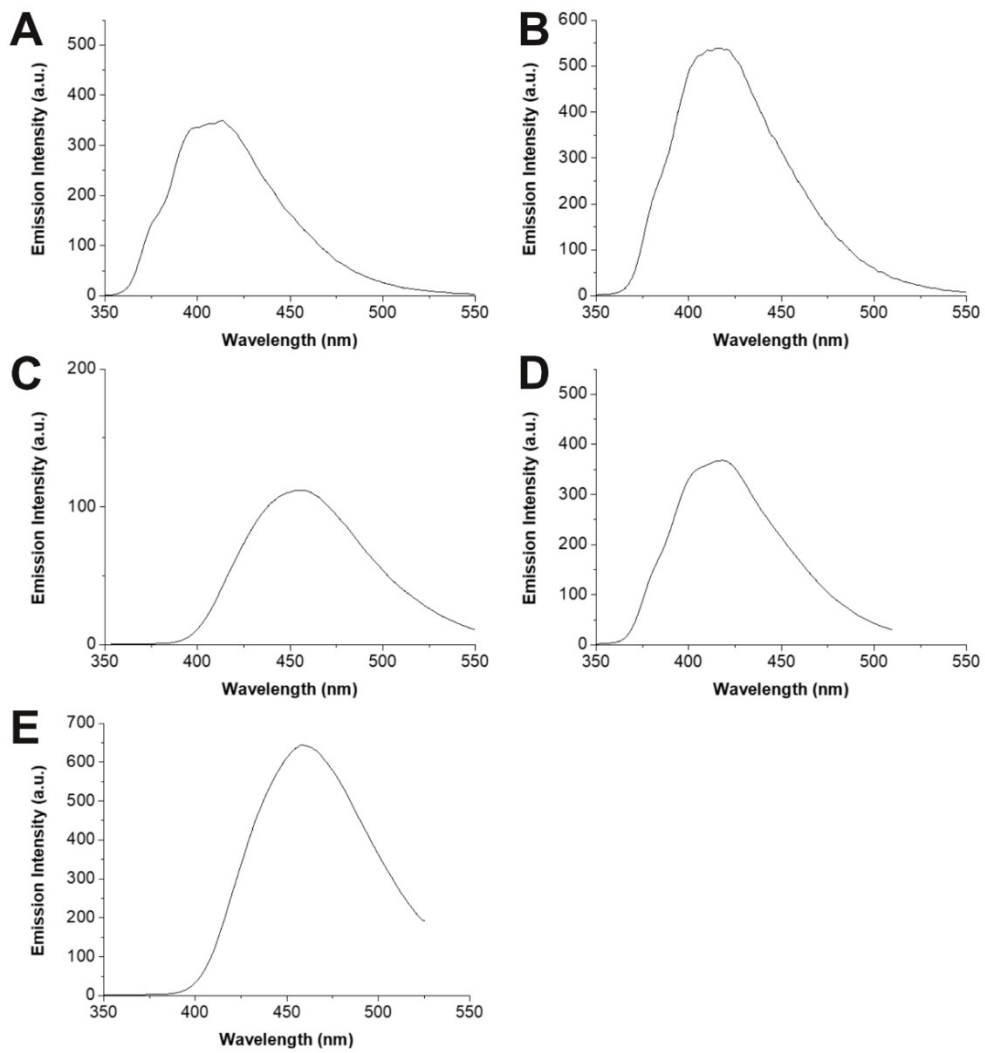


Figure S18. Fluorescence emission spectra of L1-L5 in CH_3CN solution (concentration $6.7 \cdot 10^{-5}$ mmol, quinine sulphate as reference, 25°C), (A) **L1** λ_{exc} 309 nm, slits 2.5×2.5 nm, PMT 600V, Φ 0.0820; (B) **L2** λ_{exc} 301 nm, slits 5.0×5.0 nm , PMT 600V, Φ 0.0322; (C) **L3** λ_{exc} 310 nm, slits 2.5×5.0 nm , PMT 600V, Φ 0.0310; (D) **L4** λ_{exc} 261 nm, slits 5.0×2.5 nm , PMT 600V, Φ 0.342; (E) **L5** λ_{exc} 267 nm, slits 5.0×5.0 nm , PMT 650 V, Φ 0.0266.

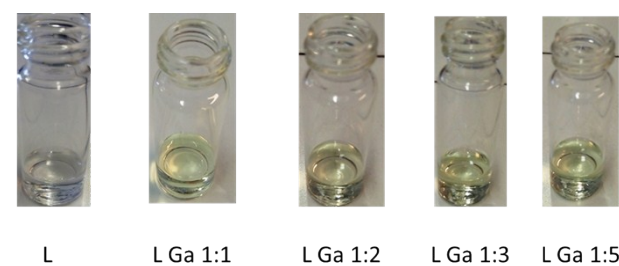
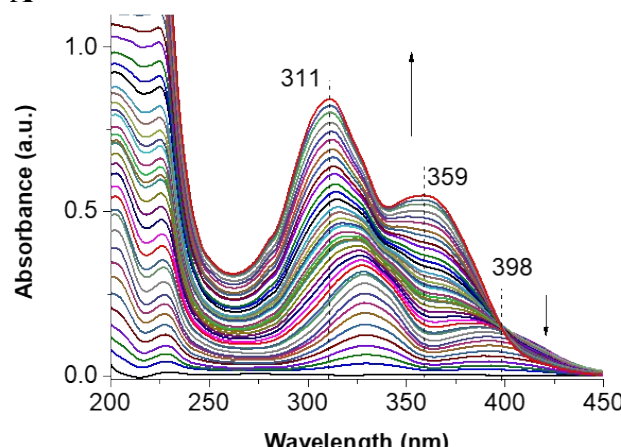
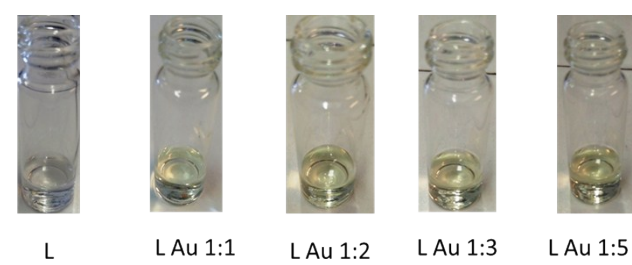
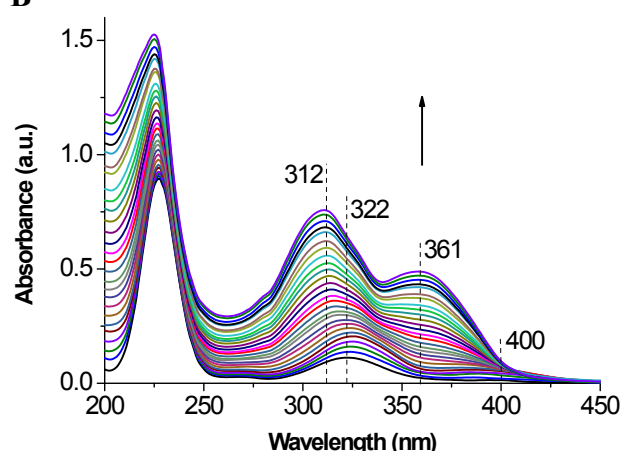
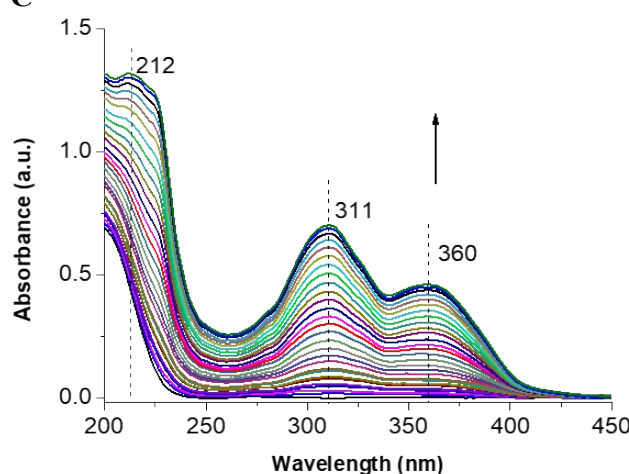
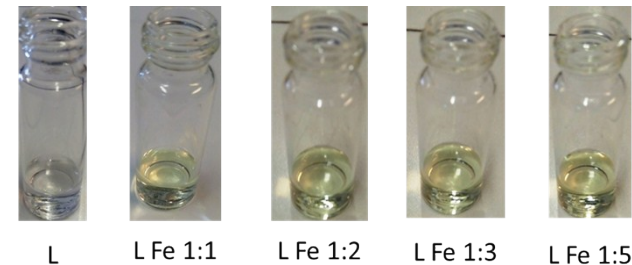
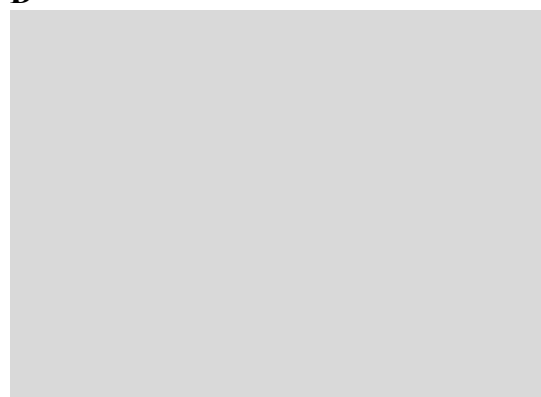
A**B****C****D**

Figure S19. Selected spectra collected during the spectrophotometric titration of Ga(III) with **L3** (**A**) (Ga(III) $5.2 \cdot 10^{-5}$ mmoles, L $6.7 \cdot 10^{-5}$ M), Au(III) with **L3** (**B**) (Au(III) $5.2 \cdot 10^{-5}$ mmoles, L $6.7 \cdot 10^{-5}$ M) and Y(III) with **L3** (**C**) (Y(III) $5.3 \cdot 10^{-5}$ mmoles, L $6.7 \cdot 10^{-5}$ M) ; NaClO₄ 0.05 M ionic strength buffer, 1 cm optical path length, 25 °C, CH₃CN solution. In the left, solutions containing ligand and metal at different molar ratios are shown to evidence the colorimetric response of the sensor. In **D** the spectrophotometrical titration of Fe(III) with **L1** is recalled for comparison.

Ga(III)-L3: by adding increasing amount of the ligand, the progressive formation of a band centred at 311 nm and a shoulder at 359 nm was observed. In addition, an isosbestic point at 398 nm was evidenced.

Au(III)-L3: the absorption maxima of Au(III) at 322 nm was gradually shifted at 312 nm by ligand addition. The presence of a shoulder at 361 nm and an isosbestic point at 400 nm were also put into evidence.

Y(III)-L3: solvated cationic core of the metal ion was progressively altered during ligand addition, as evidenced by absorption maxima shift from 200 nm to 212 nm, along with the formation of a band at 311 nm and a shoulder at 360 nm.

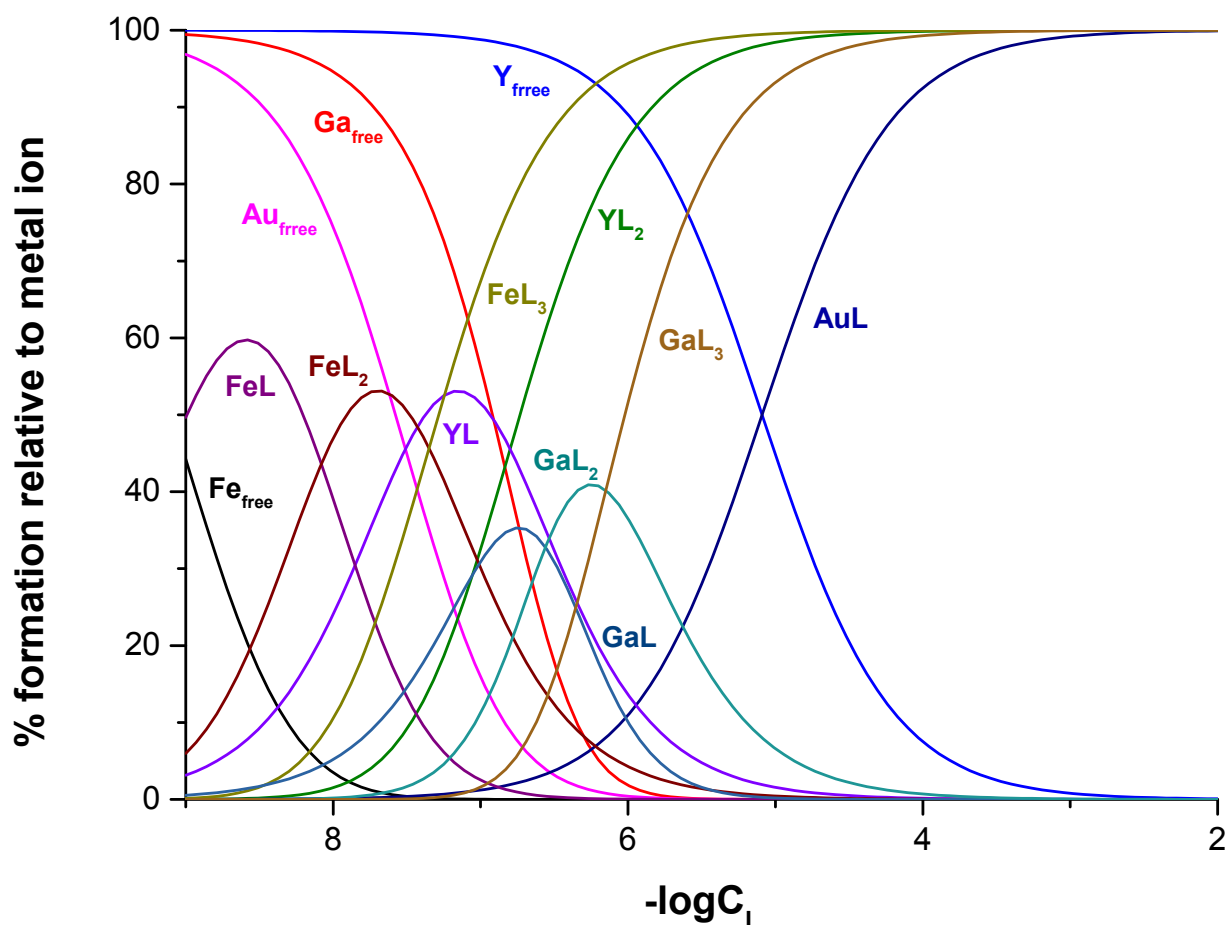


Figure S20. Calculated distribution curves for the **L3**-Fe(III)-Ga(III)-Au(III)-Y(III) system as a function of the minus logarithm of the **L3** concentration when Fe(III) is $1 \cdot 10^{-6}$ M and the other metal ions are $1 \cdot 10^{-5}$ M (**L** is **L3**)

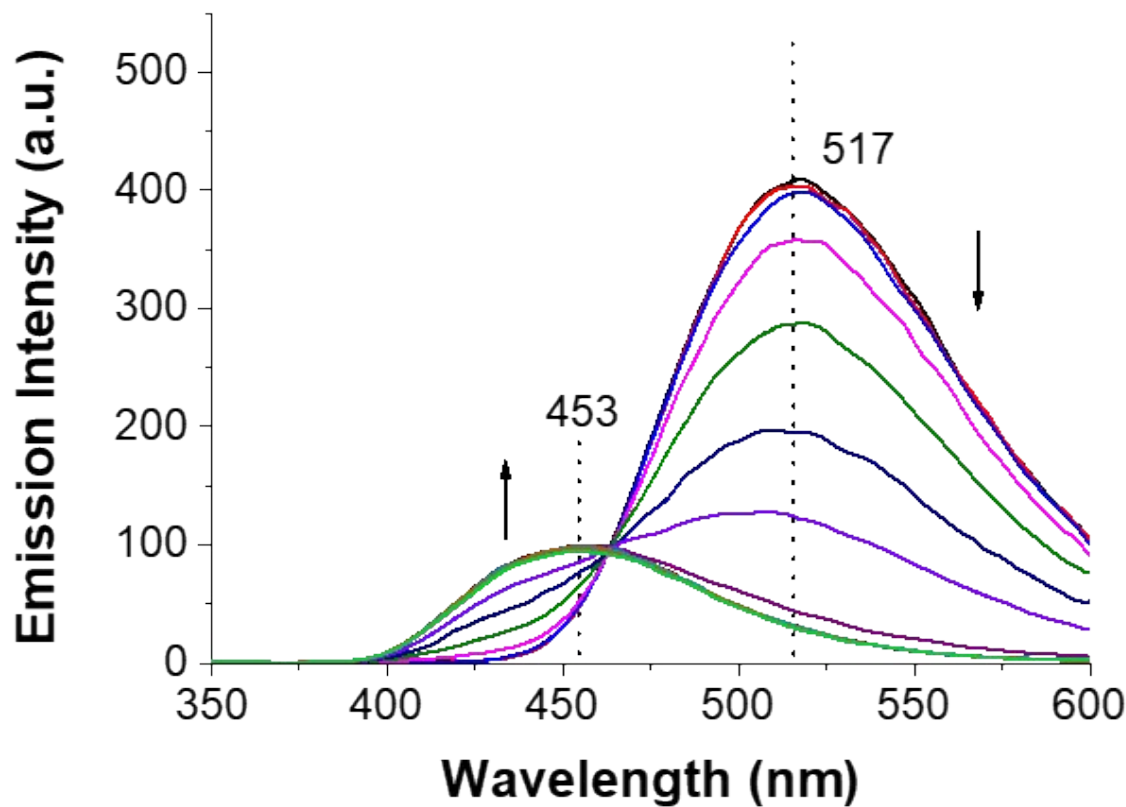


Figure S21 Selected emission spectra collected during the titration of a CH₃CN solution containing L3 ($6.7 \cdot 10^{-5}$ mmol) and Fe(III) in 1:1 molar ratio with EDTA ($2.48 \cdot 10^{-3}$ M), T 25 °C, 1 cm optical path length, λ_{exc} 310 nm, slits 2.5×5.0 nm, PMT 600V.

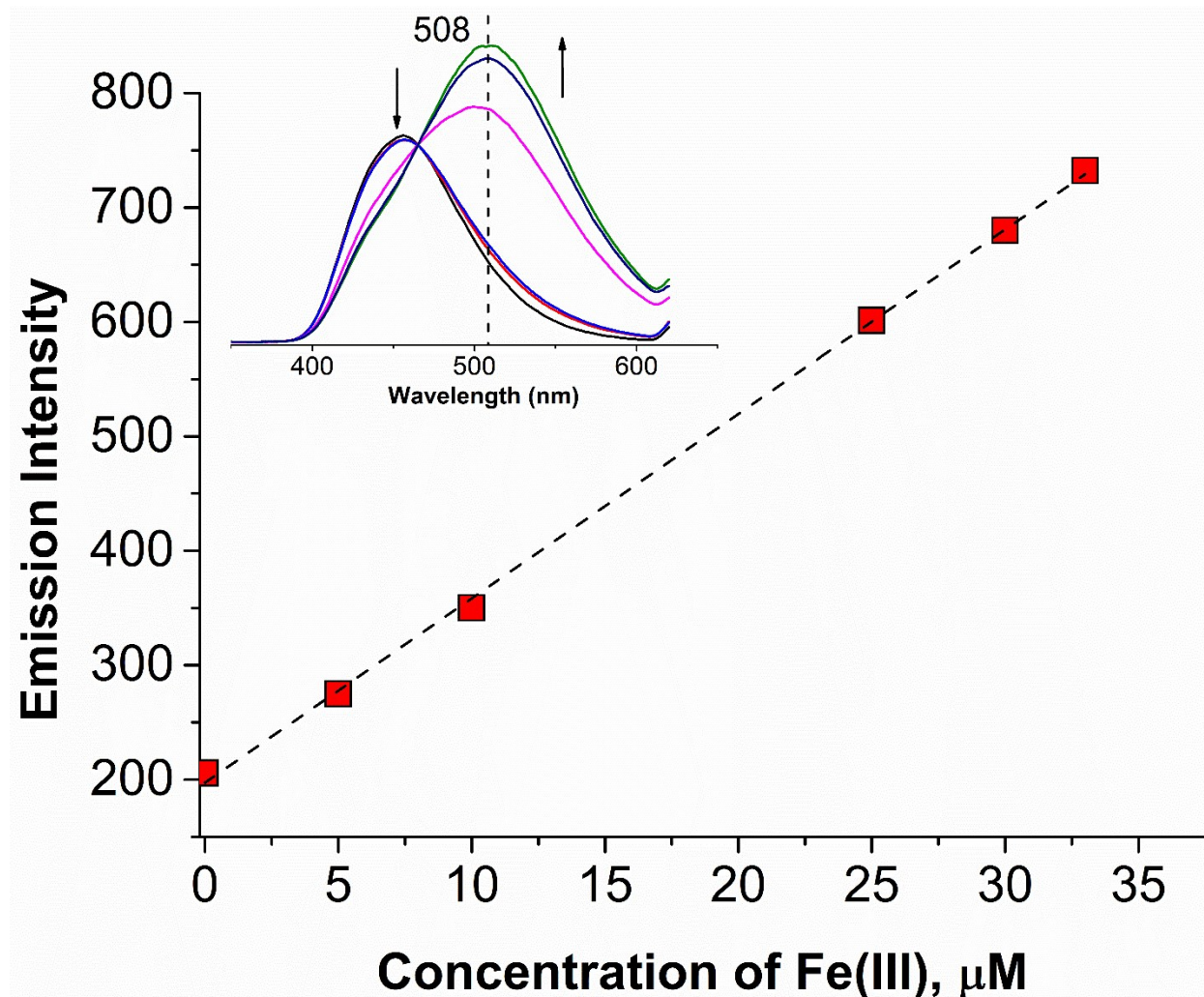


Figure S22. Linear response between emission intensity measured at 508 nm and the analytical Fe(III) concentration (**L3** concentration 35 μM , 1:1 H_2O : CH_3CN solution, T 25 $^{\circ}\text{C}$, 1 cm optical path length, λ_{exc} 310 nm, slits 2.5×5.0 nm, PMT 600V, slits 2.5×5.0 nm). $Y_{508\text{nm}} = 15.1(1)X + 203(2)$, $R^2 = 0.9999$. In the onset, the emission of **L3** and **L3** with Fe (III) in different molar ratios are reported to show the positions of the maxima.

Table S1. Selected optimized bond distances (\AA) and angles ($^\circ$) for the antiperiplanar and periplanar conformations of **L3** in acetonitrile (IEF-PCM SCRF model), and corresponding structural data for **L3**. Atom labelling scheme as in Figure S13.

Structural parameters	L3	
	Antiperiplanar	Periplanar
C8-O2	1.382	1.352
O2-C7	1.368	1.368
C7-O1	1.201	1.209
C7-C6	1.483	1.469
C6-C5	1.474	1.487
C5-N1	1.331	1.342
N1-C1	1.330	1.325
C12-O3	1.369	1.345
C13-O3	/	/
O3-C15	1.423	1.407
C8-O2-C7	123.29	124.76
O2-C7-C6	117.09	116.38
O2-C7-O1	116.64	116.23
C7-C6-C5	119.79	121.69
C6-C5-N1	114.51	115.29
C5-N1-C1	117.97	119.46
C12-O3-C15	116.78	118.73
C13-O3-C15	/	/
C7-C6-C5-N1	150.82	180.00
C8-O2-C7-O1	178.57	180.00
C11-C12-O3-C15	0.56	0.00
C14-C13-O3-C15	/	/

Table S2. Selected optimized bond distances (\AA) and angles ($^\circ$) for the low spin (LS) and high spin (HS) configurations of $[\text{Fe}(\text{L3})_3]^{3+}$ in acetonitrile (IEF-PCM SCRF model). Atom labelling scheme as in Figure S13.

	$[\text{Fe}(\text{L3})_3]^{3+}$	
	LS	HS
Fe-N1	1.994	2.133
Fe-O1	1.901	1.976
Fe-O2	1.921	2.002
Fe-N2	1.988	2.152
Fe-O3	1.902	1.992
Fe-N3	1.976	2.139
N1-Fe-O1	89.05	84.75
N1-Fe-O2	85.09	87.22
N1-Fe-N2	173.71	168.75
N1-Fe-O3	92.92	95.65
N1-Fe-N3	92.06	95.69
O1-Fe-O2	90.51	93.60
O1-Fe-N2	87.75	89.41
O1-Fe-O3	177.33	178.42
O1-Fe-N3	92.03	93.97
O2-Fe-N2	89.52	83.54
O2-Fe-O3	87.85	89.94
O2-Fe-N3	176.15	172.10
N2-Fe-O3	90.12	90.44
N2-Fe-N3	93.47	94.30
O3-Fe-N3	92.06	84.78
Fe-O1-C3	121.43	124.07
Fe-O2-C6	120.26	122.63
Fe-O3-C9	122.00	126.32
N1-C1-C2-C3	24.24	26.56
N2-C4-C5-C6	28.27	30.37
N3-C7-C8-C9	27.07	28.19
Fe-O1-C3-O4	145.25	141.06
Fe-O2-C6-O5	146.06	138.43
Fe-O3-C9-O6	146.94	143.41

Table S3. Selected optimized bond distances (\AA) and angles ($^\circ$) for the low spin (LS) and high spin (HS) configurations of $[\text{Fe}(\textbf{L3})_2(\text{H}_2\text{O})_2]^{3+}$ in acetonitrile (IEF-PCM SCRF model). Atom labelling scheme as in Figure S13.

	$[\text{Fe}(\textbf{L3})_2(\text{H}_2\text{O})_2]^{3+}$	
	LS	HS
Fe-N1	1.991	2.133
Fe-O1	1.882	1.949
Fe-O2	1.871	1.953
Fe-N2	1.982	2.131
Fe-O3	1.967	2.065
Fe-O4	1.956	2.065
N1-Fe-O1	88.63	84.96
N1-Fe-O2	86.63	88.77
N1-Fe-N2	176.53	175.16
N1-Fe-O3	93.98	93.37
N1-Fe-O4	89.33	90.04
O1-Fe-O2	92.14	93.70
O1-Fe-N2	89.01	92.64
O1-Fe-O3	175.49	176.78
O1-Fe-O4	87.09	89.18
O2-Fe-N2	90.91	86.18
O2-Fe-O3	91.68	89.04
O2-Fe-O4	175.90	177.08
N2-Fe-O3	88.53	89.22
N2-Fe-O4	93.10	94.14
O3-Fe-O4	89.27	88.06
Fe-O1-C3	121.66	123.26
Fe-O2-C6	123.49	126.46
N1-C1-C2-C3	24.62	27.47
N2-C4-C5-C6	24.72	28.69
Fe-O1-C3-O5	146.13	140.63
Fe-O2-C6-O6	150.92	145.61

Table S4. Selected optimized bond distances (\AA) and angles ($^\circ$) for the low spin (LS) and high spin (HS) configurations of $[\text{Fe}(\text{L3})(\text{H}_2\text{O})_4]^{3+}$ in acetonitrile (IEF-PCM SCRF model). Atom labelling scheme as in Figure S13.

	$[\text{Fe}(\text{L3})(\text{H}_2\text{O})_4]^{3+}$	
	LS	HS
Fe-N1	1.943	2.105
Fe-O1	1.933	2.067
Fe-O2	1.843	1.914
Fe-O3	1.974	2.072
Fe-O4	1.934	2.044
Fe-O5	1.950	2.079
N1-Fe-O1	88.75	93.98
N1-Fe-O2	92.48	86.68
N1-Fe-O3	175.03	173.59
N1-Fe-O4	95.38	92.10
N1-Fe-O5	93.54	92.91
O1-Fe-O2	90.35	87.09
O1-Fe-O3	87.38	90.59
O1-Fe-O4	175.83	173.66
O1-Fe-O5	92.35	88.20
O2-Fe-O3	84.43	87.09
O2-Fe-O4	90.03	95.03
O2-Fe-O5	173.45	175.22
O3-Fe-O4	88.52	83.20
O3-Fe-O5	89.74	82.73
O4-Fe-O5	86.84	89.74
Fe-O2-C3	123.01	127.38
N1-C1-C2-C3	23.24	24.32
Fe-O2-C3-O6	149.78	147.84

Table S5. Selected Mulliken and Natural Charges Q ($|e|$) Calculated on the low spin (LS) and high spin (HS) configurations of $[\text{Fe}(\text{L3})_3]^{3+}$ in acetonitrile (IEF-PCM SCRF model). Atom labelling scheme as in Figure S13.

Mulliken		NBO	
	$[\text{Fe}(\text{L3})_3]^{3+}$		$[\text{Fe}(\text{L3})_3]^{3+}$
	LS	HS	LS
Fe	0.642	0.981	0.826
O1	-0.344	-0.388	-0.592
O2	-0.331	-0.365	-0.590
O3	-0.344	-0.383	-0.592
N1	-0.292	-0.353	-0.452
N2	-0.309	-0.344	-0.464
N3	-0.323	-0.373	-0.470
O4	-0.195	-0.194	-0.451
O5	-0.198	-0.197	-0.454
O6	-0.196	-0.197	-0.449
			-0.453

Table S6. Selected Mulliken and Natural Charges Q ($|e|$) Calculated on the low spin (LS) and high spin (HS) configurations of $[\text{Fe}(\text{L3})_2(\text{H}_2\text{O})_2]^{3+}$ in acetonitrile (IEF-PCM SCRF model). Atom labelling scheme as in Figure S13.

Mulliken		NBO	
	$[\text{Fe}(\text{L3})_2(\text{H}_2\text{O})_2]^{3+}$		$[\text{Fe}(\text{L3})_2(\text{H}_2\text{O})_2]^{3+}$
	LS	HS	LS
Fe	0.737	1.061	0.913
O1	-0.332	-0.378	-0.575
O2	-0.338	-0.377	-0.58
O3	-0.234	-0.277	-0.843
O4	-0.224	-0.268	-0.836
N1	-0.3	-0.352	-0.457
N2	-0.321	-0.366	-0.464
O5	-0.191	-0.189	-0.448
O6	-0.187	-0.189	-0.444
			-0.447

Table S7. Selected Mulliken and Natural Charges Q ($|e|$) Calculated on the low spin (LS) and high spin (HS) configurations of $[\text{Fe}(\text{L3})(\text{H}_2\text{O})_4]^{3+}$ in acetonitrile (IEF-PCM SCRF model). Atom labelling scheme as in Figure S13.

	Mulliken		NBO	
	$[\text{Fe}(\text{L3})(\text{H}_2\text{O})_4]^{3+}$		$[\text{Fe}(\text{L3})(\text{H}_2\text{O})_4]^{3+}$	
	LS	HS	LS	HS
Fe	0.753	1.121	0.949	1.533
O1	-0.215	-0.275	-0.818	-0.909
O2	-0.355	-0.375	-0.572	-0.651
O3	-0.225	-0.281	-0.830	-0.916
O4	-0.208	-0.275	-0.806	-0.911
O5	-0.230	-0.274	-0.838	-0.916
N1	-0.334	-0.374	-0.452	-0.572
O6	-0.178	-0.177	-0.436	-0.437

Table S8. calculated concentrations of each complex species for systems containing L3-Fe(III)-Au(III) (**A**), L3-Fe(III)-Y(III) (**C**), L3-Fe(III)-Ga(III) (**E**) and L3-Fe(III)-Au(III)-Y(III)-Ga(III) (**G**) at 1×10^{-5} M, L3-Fe(III)-Au(III) (**B**), L3-Fe(III)-Y(III) (**D**), L3-Fe(III)-Ga(III) (**F**) and L3-Fe(III)-Au(III)-Y(III)-Ga(III) (**H**) at metal concentration 1×10^{-6} M and ligand concentration at 1×10^{-6} M.

conditions	point 1						
total Fe	1.000E-05	total Fe	1.000E-06	total Fe	1.000E-05	total Fe	1.000E-06
total Au	1.000E-05	total Au	1.000E-06	total Y	1.000E-05	total Y	1.000E-06
total L	1.000E-05						
p(Fe)	(set pX)						
p(Au)	(set pX)	p(Au)	(set pX)	p(Y)	(set pX)	p(Y)	(set pX)
p(L)	(set pX)						
results	concn./M	results	concn./M	results	concn./M	results	concn./M
free Fe	2.06850E-06	free Fe	1.16495E-15	free Fe	2.40934E-06	free Fe	2.56422E-15
free Au	9.99683E-06	free Au	5.53380E-07	free Y	9.32729E-06	free Y	1.86925E-10
free L	2.57458E-09	free L	6.56016E-06	free L	2.19831E-09	free L	5.03967E-06
AuL	3.16642E-09	AuL	4.46620E-07	YL	6.63506E-07	YL	3.04838E-08
FeL	5.97534E-06	FeL	8.57474E-12	YL ₂	9.20309E-09	YL ₂	9.69329E-07
FeL ₂	1.84955E-06	FeL ₂	6.76292E-09	FeL	5.94274E-06	FeL	1.44996E-11
FeL ₃	1.06604E-07	FeL ₃	9.93228E-07	FeL ₂	1.57063E-06	FeL ₂	8.78534E-09
				FeL ₃	7.72972E-08	FeL ₃	9.91200E-07

A

B

C

D

conditions	point 1	conditions	point 1
total Fe	1.000E-06	total Fe	1.000E-05
total Ga	1.000E-06	total Ga	1.000E-05
total L	1.000E-05	total L	1.000E-05
p(Fe)	(set pX)	p(Fe)	(set pX)
p(Ga)	(set pX)	p(Ga)	(set pX)
p(L)	(set pX)	p(L)	(set pX)
results	concn./M	results	concn./M
free Fe	4.50394E-15	free Fe	2.13322E-06
free Ga	4.12927E-10	free Ga	9.86348E-06
free L	4.17438E-06	free L	2.49591E-09
Gal	9.47252E-09	Gal	1.35288E-07
Gal ₂	1.43568E-07	Gal ₂	1.22599E-09
Gal ₃	8.46546E-07	Gal ₃	4.32233E-12
FeL	2.10953E-11	FeL	5.97398E-06
FeL ₂	1.05871E-08	FeL ₂	1.79263E-06
FeL ₃	9.89392E-07	FeL ₃	1.00166E-07

E

F

conditions	point 1	conditions	point 1
total Fe	1.000E-05	total Fe	1.000E-06
total Au	1.000E-05	total Au	1.000E-06
total Y	1.000E-05	total Y	1.000E-06
total Ga	1.000E-05	total Ga	1.000E-06
total L	1.000E-05	total L	1.000E-05
p(Fe)	(set pX)	p(Fe)	(set pX)
p(Au)	(set pX)	p(Au)	(set pX)
p(Y)	(set pX)	p(Y)	(set pX)
p(Ga)	(set pX)	p(Ga)	(set pX)
p(L)	(set pX)	p(L)	(set pX)
results	concn./M	results	concn./M
free Fe	2.41057E-06	free Fe	3.20511E-15
free Au	9.99730E-06	free Au	6.34739E-07
free Y	9.32764E-06	free Y	2.16481E-10
free Ga	1.00000E-05	free Ga	9.99999E-07
free L	2.19710E-09	free L	4.67743E-06
AuL	2.70229E-09	AuL	3.65261E-07
FeL	5.94251E-06	FeL	1.68210E-11
FeL ₂	1.56971E-06	FeL ₂	9.45926E-09
FeL ₃	7.72090E-08	FeL ₃	9.90524E-07
YL	6.63164E-07	YL	3.27662E-08
YL ₂	9.19328E-09	YL ₂	9.67017E-07
YGaL	1.12621E-12	YGaL	5.56449E-15
YGaL ₂	8.98401E-15	YGaL ₂	9.45003E-14
YGaL ₃	2.78818E-17	YGaL ₃	6.24369E-13

G

H